Long-term EEJ variations by using the improved EE-index

著者	Fujimoto Akiko, Uozumi Teiji, Abe Shuji, Matsushita Hiroki, Imajo Shun, Ishitsuka Jose K., Yoshikawa Akimasa
journal or publication title	Sun and Geosphere
volume	11
number	1
page range	37-47
year	2016
URL	http://hdl.handle.net/10228/00007447

Long-term EEJ variations by using the improved EE-index

Akiko Fujimoto[1], Teiji Uozumi[1], Shuji Abe[1], Hiroki Matsushita[2], Shun Imajo[2], Jose K. Ishitsuka[3], Akimasa Yoshikawa[1]

[1] International Center for Space Weather Science and Education, Kyushu University, Japan
[2] Department of Earth and Planetary Sciences, Kyushu University, Japan
[3] Observatorio de Huancayo, Instituto Geofisico del Peru, Peru

E mail (fujimoto@icswse.kyushu-u.ac.jp).

Accepted 8 January, 2016

Abstract: In 2008, International Center for Space Weather Science and Education, Kyushu University (ICSWSE) proposed the EE-index, which is an index to monitor the equatorial geomagnetic phenomena. EE-index has been improved with the development of the MAGnetic Data Acquisition System and the Circum-pan Pacific Magnetometer Network (MAGDAS/CPMN) and the enormous archive of MAGDAS/CPMN data over 10 years since the initial article. Using the improved EE-index, we examined the solar cycle variation of equatorial electrojet (EEJ) by the time series analysis for EUEL (one part of EE-index) at Ancon in Peru and the solar activity from September 18, 1998 to March 31, 2015. We found that the long-term variation of daily EEJ peak intensity has a trend similar to that of F10.7 (the solar activity). The power spectrum of the daily EEJ peak has clearly two dominant peaks throughout the analysis interval: 14.5 days and 180 days (semi-annual). The solar cycle variation of daily EEJ peak correlates well with that of F10.7 (the correlation coefficient 0.99). We conclude that the daily EEJ peak intensity is roughly determined as the summation of the long-period trend of the solar activity resulting from the solar cycle and day-to-day variations caused by various sources such as lunar tides, geometric effects, magnetospheric phenomena and atmospheric phenomena. This work presents the primary evidence for solar cycle variations of EEJ on the long-term study of the EE-index.

Keywords: EE-index, equatorial electrojet, MAGDAS/CPMN, space weather

Introduction

In 2008, International Center for Space Weather Science and Education, Kyushu University (ICSWSE) proposed the monitoring index for equatorial electrojet (EEJ) by using MAGnetic Data Acquisition System and the Circum-pan Pacific Magnetometer Network (MAGDAS/CPMN) (Yumoto and the CPMN group, 2001; Yumoto and the MAGDAS group, 2006, 2007) data, which we called as EE-index (Uozumi et al., 2008). EE-index has been developed with the object of separating the magnetic disturbances in the equatorial region into the global and local magnetic variations and also monitoring quantitatively various electromagnetic phenomena in real time. The first paper (Uozumi et al., 2008) of EE-index provided one month MAGDAS/CPMN magnetic field data to explain the algorithm of the index. EE-index consists of two parts: EDst and EUEL index. Uozumi et al. (2008) defined that EDst (the equatorial disturbance storm time) index represents the global magnetic variation including disturbances in the equatorial region caused by sudden storm commencement (SSC) and ring current and a part of magnetospheric polar disturbances such as substorms and DP2 effects. EUEL index is given by the subtraction of EDst index from the relative H-component (ERs, the definition is given in the Material and methods). EUEL shows the total overhead currents involved in EEJ/Sq at the equatorial region without the global common magnetic effects changing moment by moment. The positive and negative of EUEL index indicate the magnetic effects generated by eastward and westward currents at the concerned station, respectively.

The EEJ is known to flow eastward in a narrow latitude band (~±3°) along the magnetic equator. Therefore, its magnetic contribution is expected to overlap the planetary Sq effects near the magnetic equator. When a single latitude chain of stations is considered, it appears that the EEJ effect superimposes that of the planetary Sq in a certain latitude band across the magnetic equator (Onwumechili, 1967; Fambitakoye and Mayaud, 1976a, 1976b; Fambitakoye, Mayaud, and Richmond, 1976).

In the early study of EEJ, researchers have revealed the morphology of EEJ during the quiet time in the terms of the variation of the "daily range" or "regular daily variation". These variables provide the total overhead currents on the dip-equator and divide into two components: EEJ and Sq currents. Chapman and Raja Rao (1965) presented the daily range as the difference between the midday mean and the midnight mean on a given day of the northward magnetic component. The regular daily variation is defined as the deviation between a given instant and the night level (zero level). Fambitakoye and Mayaud (1976a) determined the zero level by interpolating linearly between two midnights neighboring the day considered.

The manner of estimating the daily variation of EEJ and Sq current magnetic effect is strongly supported by the fact of the daytime ionospheric wind dynamo theory. It is well known that the circulation of currents in

the lower ionosphere, denoted as the daytime ionospheric wind dynamo, causes EEJ and Sq currents. Since the source of the ionospheric dynamo is the solar daily radiations, the magnetic effect of this dynamo is generally negligible during the nighttime. Additionally, the magnetic effects attributed the magnetospheric current systems (e.g., the Chapman-Ferraro current on the magnetopause and the ring-current, which are estimated through the Dst index) exist during the daytime as well as the nighttime. Thus, during the quiet time it is acceptable to definition of the daily range or the regular daily variation. However, they are not suitable for the geomagnetic disturbed time such as during magnetic storms because the nightside magnetic variability is not stable or constant.

The further understanding of EEJ mechanisms needs to separate the daily range/regular daily variation into the EEJ and Sq current magnetic effects. To isolate the EEJ effect from the planetary Sq, different approaches are used, depending on the workers and on available datasets. Some will use pairs of stations located at the same longitude (Rastogi, Chandra, and Yumoto, 2013). One station of the pair is chosen at the magnetic equator, and the other must be chosen enough far away from the EEJ influence (hereafter called pair stations method). The weakness of this approach relies on the fact that the planetary Sq also varies as function of latitudes across the magnetic equator. Hamid et al. (2014) analyzed EUEL index (which is one part of EE-index) to examine the relationship between EEJ and Sq, with the CM4 global current model (Sabaka, Olsen, and Purucker, 2004) to minimize the latitudinal uncertainty of EEJ/Sq. More accurate approach is the use of a latitude chain, enough extended in latitude to include both the latitude profiles of the Sq and the EEJ effects (Rigoti et al., 1999). In that case, the Sq is represented by the background signal, which can be fitted and removed.

Based on the several manners described above, EEJ has been studied by many researchers in order to explain the mechanisms of EEJ. Some features of EEJ variations have been revealed since its discovery at Huancayo in Peru (Forbes, (1981) for a review). The following characteristics are provided by the ground-based magnetometer data: diurnal, semi-diurnal and semi-annual variability (Chapman and Raja Rao, 1965; Rastogi, Alex, and Patil, 1994), day-to-day variations (Fambitakoye and Mayaud, 1976b; Kane and Trivedi, 1980; Doumouya et al., 1998), counter equatorial electrojet (CEJ), the dependence of solar radio flux (F10.7) (Rastogi and Iyer, 1976; Rastogi, Alex, and Patil, 1994), latitudinal structure (Rigoti et al., 1999), local time and longitudinal dependence of EEJ (Doumouya et al., 2003).

These evidences have been provided by the analysis of the magnetic quiet EEJ. Since there is no significant magnetic variation at the midnight during the magnetic quiet time, the past researchers have used the constant nighttime level to determine the magnetic variations affected by the EEJ/Sq currents (Chapman and Raja Rao, 1965). Many studies of quiet-time EEJ variations have been reported over the past decades, whereas the disturbance-time EEJ variability has never enough been studied. The traditional determination manner of the daily magnetic variations is useless for the magnetic disturbance time, for example, magnetic storms. It is because we cannot properly consider the magnetic field variations affected by the ring current during the magnetic storms.

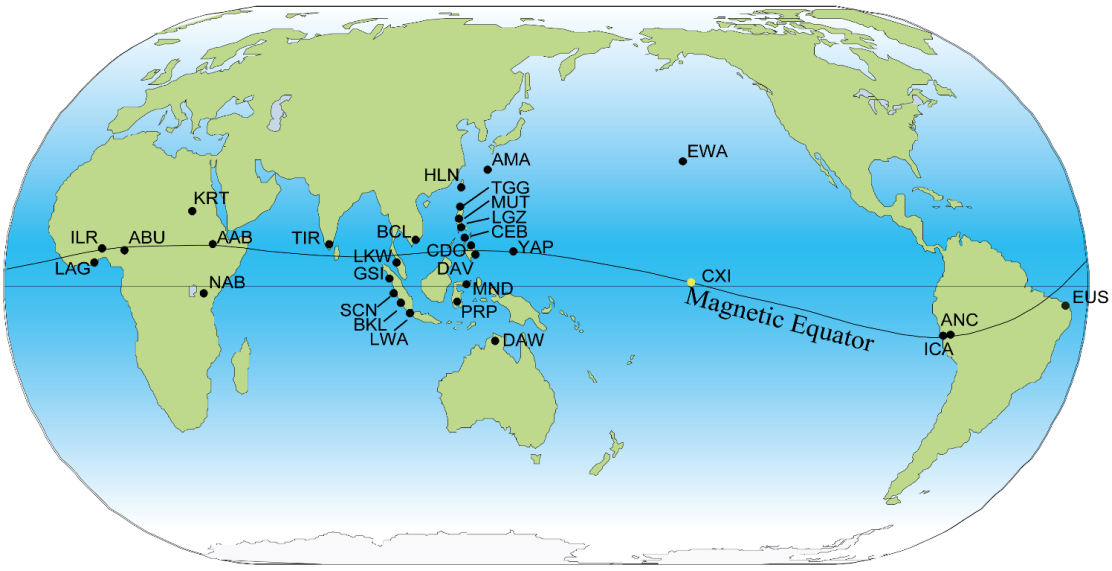

Figure 1: A map of MAGDAS stations used in this paper. The stations marked with the black filled circle except for CXI (yellow filled circle) are used in the EE-index procedure. CXI is only used for validating whether low-latitude stations can be used as the proxy of magnetic field intensity at the dip-equator stations along the same longitude. The detailed descriptions are given in the section of Materials and methods. CXI belongs to the Ocean Hemisphere network Project (OHP), University of Tokyo.

We also believe the importance of the study on geomagnetic disturbances as well as on quiet time magnetic variations. For example, the equatorial plasma bubble in the night side is involved with magnetic storms. In order to understand the mechanisms of plasma bubble, we need quantitatively to analysis the equatorial magnetic variation during the magnetic disturbance time as well as the quiet time. Today human activity and society extend to the space. The plasma bubble is well known to cause the communication failure between satellites and ground stations. The monitoring of space weather environment is needed to allow us the safety life involving the space weather. ICSWSE provides the real time EE-index on our web site, in terms of the monitoring of space weather environment. The consecutive monitoring of equatorial magnetic variations requires an indicator unaffected by the magnetospheric environment.

In order to achieve the objective of space weather monitoring, the possible solution is the development of the daily range method since the appropriate station pair may not always exist for applying to two stations pair method. We use the nighttime magnetic variations as the dynamic reference base level by using the multiple equatorial magnetometer observations spread through the longitude direction. The advantage of this new method is that it is possible to monitor the equatorial magnetic field variations changing from moment to moment. Additionally we can evaluate the equatorial magnetic variation with the same ruler regardless of magnetic environment (quiet/disturbance) of the magnetosphere.

Many past studies (utilizing the daily range method and the pair stations method) discussed the mechanism or morphology of the quiet time EEJ, due to the aforementioned reasons. Moreover the superposed EEJ variations in past papers showed the relationship between the EEJ intensity and UT/LT (Universal Time/Local Time). However few reports have been issued in terms of the time series analysis for the long-term comparison between the EEJ variations and solar activity/magnetospheric/atmospheric phenomena because the successive time information is removed from the data. In contrast, our new index enables us to study the time series analysis for revealing the relation between EEJ and 11-year solar cycle/climate changes through several decades with high time resolution. EE-index has been improved in terms of using long-term MAGDAS/CPMN archives and multiple equatorial magnetometer data (Figure 1) since this index was produced in 2008. In the present paper, we describe the improvement of EE-index and introduce the application example as the long-term EEJ variations compared with the solar activity.

Materials and methods

EE-index is divided into the global and local components named as EDst and EUEL, respectively.

$$EEindex = EDst + EUEL \quad (1)$$

EDst represents the simultaneous magnetic field variations appearing throughout the entire magnetic equator. EUEL shows the localized variations in the magnetic field at each individual station. The process of obtaining the primary EE-index (EDst and EUEL) is summarized as follows: (a) use the dip-equatorial H component in the time series of magnetometer data (the data sampling time is one minutes, the MAGDAS/CPMN magnetometer stations are located at within ± 3 degrees in latitude), (b) calculate the relative magnetic field ($ER_S(m)$, S and m indicate indicate the station and time, respectively): obtained by subtraction of the median value throughout the whole data used in the procedure from the original H component data for each individual stations, (c) determine EDst using the averaged night time magnetic field $ER_S(m)|_{LT=18\text{-}06}$, all selected stations are located between LT = 18 and 06:

(2)

Where $N(m)|_{LT=18\text{-}06}$ indicates the number of stations located in the nighttime sector (LT = 18-06). Considering that the nightside ionospheric conductivity is small compared to dayside conductivity, the localized ionospheric current is limited in the nighttime sector. Consequently, the observed magnetic field at the nightside is mostly the variations resulted in the global phenomena such as the equatorial ring current. (d) Finally get $EUEL_S(m)$ by subtracting 6-h running average of EDst(m) (labeled $EDst_{6h}(m)$) from $ER_S(m)$ for each individual stations. The positive and negative of $EUEL_S(m)$ represent the magnetic variations produced by eastward currents and westward currents, respectively. We expressly define the positive of $EUEL_S(m)$ as $EU_S(m)$ and negative of $EUEL_S(m)$ as $EL_S(m)$.

As described in Uozumi et al. (2008), the fundamental algorithm of EE-index is an improved method of the traditional manner as referred to Chapman and Raja Rao (1965). That is the daily EEJ intensity is provided by the derivation of the midnight magnetic field value from the time series of magnetic field value. In the traditional method, the midnight magnetic field value is adopted to the reference base level with the hypothesis that is the midnight value is stable for an entire single day. Rastogi and Iyer (1976) showed that around midnight the magnetic field remained constant during a low sunspot year and changeable during a high sunspot year. This suggests that the fixed reference value is an unsuitable parameter for determining the total intensity of EEJ variations. In our method, however, the reference level varies with time. In order to obtain the reference level value, the multiple dip-equatorial stations, which are spread worldwide, are used in our procedure: 4 stations in Uozumi et al. (2008).

Uozumi et al. (2008) left the lower accuracy in the determination of the reference level due to few stations used in the procedure. Thus we tried to improve matters in terms of using more stations than Uozumi et al. (2008) for the calculation of EDst. The number of MAGDAS/CPMN network stations has increased since the first EE-index paper was published

in 2008. Now there are 12 dip-equator stations covering whole longitudinal sectors (within ±3 degrees in latitude). The past EE-index in Uozumi et al. (2008) used at most two-nightside stations. Consequently EDst remains of the disturbed magnetic field variations such as the substorm positive bay observed during the substorm. The reference base level is calculated by using the dip-equatorial data obtained from at most 10-nightside stations and at least 2-nightside stations. The EDst in the renewed EE-index monitors the global magnetic disturbed variations with higher accuracy than Uozumi et al. (2008).

The most critical problem for operating the EE-index is that there are few dip-equatorial MAGDAS/CPMN stations in the Pacific Ocean as shown in Figure 1. We assumed that the magnetic field at a low-latitude station estimates the equatorial magnetic field along the same longitudinal line during the nighttime sector. It is because the nightside ionospheric conductivity is almost equivalent between the dip-equator and the low latitude, whereas there is significant difference between two latitudinal regions for the dayside conductivity. In order to validate this assumption, we examined the relationship of the magnetic field intensity between CXI (CXI data is provided from the Ocean Hemisphere network Project (OHP), University of Tokyo) as the dip-equatorial station and EWA as the low-latitude station. The 1-min. H component in magnetic field data from 1999 January 1 to 2000 December 31 was analyzed. We calculated the equatorial estimated H component value ($H_{equator}$) from H component observed at EWA station (H_{EWA}) by using the correcting function for the latitudinal effect,

$$H_{equator}=H_{EWA} / \cos(\Phi_{EWA}) \quad (3)$$

Where Φ_{EWA} is the geomagnetic latitude (gmlat) value of *EWA* station. We found the good correlation between the observed magnetic field (H_{CXI}) at CXI and the $H_{equator}$ value estimated from H_{EWA} with the correlation coefficient 0.83 (not shown). The function of the linear regression analysis between H_{CXI} and $H_{equator}$ is

$$H_{CXI} = 1.03 \text{ X } H_{equator} - 7.05 \quad (4)$$

The slope value of the function suggests that the nighttime magnetic field is controlled by the current system such as the ring current and the magnetospheric tail current which widely influence along the latitude, without the variations affected by the ionospheric current. Figure 2 shows the magnetic field data at CXI and EWA with SYM-H (provided by World Data Center (WDC) for Geomagnetism Kyoto University). The SYM-H is used to show the global magnetic disturbance such as the magnetic storm in this paper. As shown in Figure 2, there are similar variabilities between CXI and EWA during the nighttime. We conclude that the equatorial estimated H component from the low-latitude H component is acceptable to the magnetic field intensity at the equator.

As described above, the magnetic field data obtained from low-latitude stations can be used as the proxy of the intensity at the dip-equatorial stations along the same longitude. Now it must be noted that this estimation is applied to the low latitude stations, whereas the magnetic field of dip-equatorial and off-dip stations are used without the latitudinal correction. Thus, the former is the magnetic field variations at gmlat = 0 and the latter is at gmlat ≠ 0. This process consequently results in two different quantities. In order to avoid this matter, we assume that the equatorial estimated magnetic field intensity can be calculated from data recorded at any station in less than low latitude (<± 25 degrees). That is, the equation (3) would be applied to the magnetic field data at not only low latitude stations (located within |10-25| degrees in latitude) but also off–dip stations (within |3-10| degrees in latitude) and dip-equatorial stations (< |3| degrees in latitude). Hence,

$$H_{dip}=H_S / \cos(\Phi_s) \quad (5)$$

Where *S* indicates any station located within ±25 degrees in latitude, H_{dip} means the H component value at gmlat = 0. The division value on the right side ($1/\cos(\Phi_S)$) is less than 1.1 when the latitude value is less than 25. This means that the value estimated by the equation (5) has errors with at most 10% for the lower latitude. The errors decrease with decreasing latitudinal value.

The equation (5) applies to the calculation of EDst index. Dst index is determined by the same manner in terms of the latitudinal correction of H-component magnetic field. This latitudinal correction applies to the standardization of the low-latitudinal magnetic field data into the dip magnetic field value. The correction is appropriate since the magnetic effect during magnetic storms is assumed to be affected by the ring current existing far from the surface of the earth. EDst index indicates the magnetic effect of the magnetospheric currents including the ring current. We believe that the latitudinal correction is useful to estimate the magnetospheric currents.

In the past, the EE-index assumed that the magnetic field value at the inside the narrow channel (<±3 degrees in latitude) of the EEJ band as the magnetic field intensity at gmlat = 0. Using the improved assumption explained above, we obtain the estimated magnetic field intensity on the dip equator from any magnetometer station not exactly located on dip-equator (that is, all of MAGDAS/CPMN stations). This means that EDst is calculated by using 29 MAGDAS/CPMN stations located from dip-equator to low-latitude: 12 dip-equatorial (the narrow channel), 7 off-dip and 10 low-latitude stations (Table 1, except for CXI). The latest EE-index procedure is as follows:

Step1. Use the magnetometer data obtained from the MAGDAS/CPMN stations located within ±25 degrees in latitude, with one minute resolution

Step2. Calculate the relative magnetic field for each individual station: $ER_S(m)$

Step3. Estimate the dip-equatorial magnetic field value (gmlat = 0) by applying the equation (5) for each individual stations during the nighttime sector: $ER_{dip}(m)|_{LT=18\text{-}06}$ (this is the estimated

value on the dip equator from any station located at LT = 18-06)

Step4. Determine EDst(m) by averaging the dip-equatorial estimated magnetic field $ER_{dip}(m)|_{LT=18\text{-}06}$ during the night time

Step5. Convert EDst(m) into $EDst_S(m)$ for each individual station by correcting the latitudinal effect

Step6. Get $EUEL_S(m)$ by subtracting $EDst_{S,6h}(m)$ from $ER_S(m)$ for each individual station

Here we provide the comparison of the results calculated from three method (the daily range, EE-index: EDst and EUEL indices and the pair stations method), in order to suggest that EE-index is the useful tool on the monitoring of equatorial magnetic variations. Figure 3 and 4 show each behavior of all methods for the quiet and disturbance time magnetic variations, respectively. Note that we use the manner of Chapman and Raja Rao (1965) as the determination of the daily range. The primary objective of providing these figures is to show the difference between the daily range method and EE-index approach, caused by the different manner of reference level: the stable or drastic night magnetic field references. The presented magnetic field data are obtained from two stations of MAGDAS network. One is DAV (-1.02 gmlat) as the dip station, the other is MND (-6.91gmlat) as the off-dip station. The period

Table 1: Geographical and geomagnetic coordinates of the stations. The latest EE-index uses the stations except for CXI. The used stations will be changed in the future due to operating MAGDAS/CPMN observations.

station		geographic		geomagnetic	
Name	code	latitude(°)	longitude(°)	latitude(°)	longitude(°)
Addis Abeba	AAB	9.04	38.77	0.18	110.47
Abuja	ABU	8.99	7.39	-1.53	79.4
Amami Oshima	AMA	28.17	129.33	21.11	200.88
Ancon	ANC	-11.77	282.85	0.77	354.33
Bac Lieu	BCL	9.3	105.71	-0.66	177.96
Bengkulu	BKL	-3.8	102.31	-15.13	173.6
Cagayan De Oro	CDO	8.4	124.63	-1.1	196.66
Cebu	CEB	10.36	123.91	2.53	195.06
Davao	DAV	7	125.4	-1.02	196.54
Darwin	DAW	-12.41	130.92	-21.91	202.81
Eusebio	EUS	-3.88	321.57	-3.64	34.21
Ewa Beach	EWA	21.3	202	21.67	269.52
Gunung Sitoli	GSI	1.29	97.61	-7.53	169.49
Hualien	HLN	23.9	121.55	16.86	193.05
Ica	ICA	-14.09	284.26	-1.56	356.16
Ilorin	ILR	8.5	4.68	-1.82	76.8
Khartoum	KRT	15.3	32.32	5.69	103.8
Lagos	LAG	6.4	3.27	-3.04	75.33
Legazpi	LGZ	13.1	123.74	3.54	195.56
Langkawi	LKW	6.3	99.78	-2.32	171.29
Liwa	LWA	-5	104.06	-16.19	175.33
Manado	MND	1.44	124.84	-6.91	196.06
Muntinlupa	MUT	14.37	121.02	6.79	192.25
Nairobi	NAB	-1.1	36.48	-10.65	108.18
Pare Pare	PRP	-3.6	119.4	-12.38	190.75
Sicincin	SCN	-0.5	100.3	-12.11	171.66
Tuguegarao	TGG	17.66	121.76	10.26	193.05
Trivandrum	TIR	8.48	76.95	-0.37	149.11
Yap	YAP	9.5	138.08	1.49	209.06
Christmas Island	CXI	1.91	202.51	2.64	273.89

demonstrated in Figure 2 and 3 is 12th June 2010 and 15th February 2012 in local time (125 degrees east longitude), respectively. On 12th June 2010, the magnetosphere is quiet: Kp index=0 and International Q-Days (Q1: the most quiet day in the month). On 15th February 2012, the magnetosphere spent disturbance time: Kp~3-4, International D-Days (D1: the most disturbance day in the month). Kp, Q-days and D-days are obtained from GFZ German Research Centre for Geosciences.

For the magnetic quiet time shown in Figure 3(b), there is no remarkable difference between the daily range method (grey solid line) and EUEL (red dashed line) of EE-index during daytime. The result is reasonable because the reference zero level of EE-index (EDst value) is almost stable during the daytime in the present event and there is little difference between two midnights neighboring the day considered for the daily range method. On the other hand, the slight difference exists during the nighttime. EUEL value of EE-index during the nighttime (local time = 21-24) shows zero since EDst (green solid line) estimates successfully the magnetic effect of the magnetospheric currents. In both methods, the CEJ is clearly found around the evening.

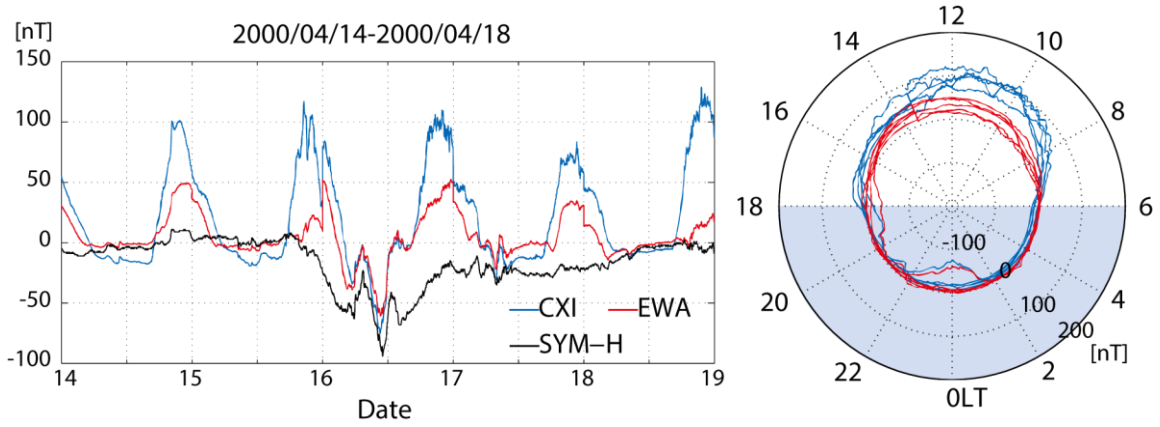

Figure 2: The magnetic field (H component) at CXI and EWA with SYM-H. EWA data are corrected for the latitudinal effect. The left panel shows the time series data and the right panel illustrates the magnetic field variations in the polar coordinate viewed from north during April 14 – 18, 2000.

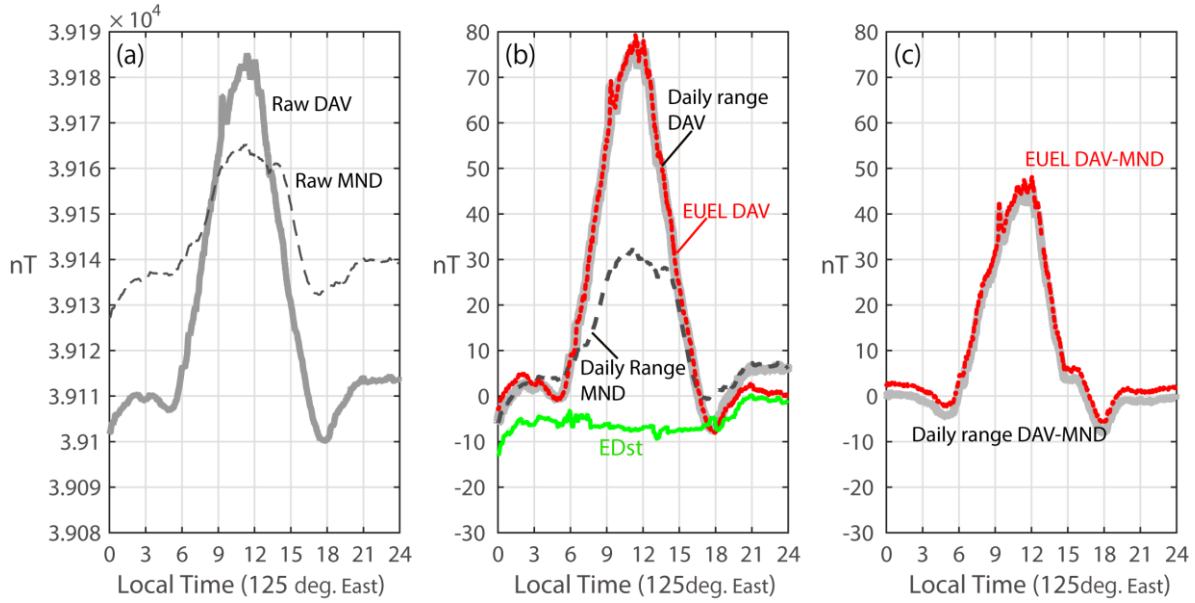

Figure 3: Schematic illustration of the daily range method, EE-index and two pair stations method during the geomagnetic quiet time on 12th June 2010 in the local time (125 degrees east longitude), from June 11 (1540 UT) to 12 (1539 UT) 2010. DAV is a dip-equator station and MND is an off-dip station. (a) raw magnetic field data at DAV and MND, (b) the daily range of DAV (grey solid line) and MND (grey dashed line), EUEL variation of DAV (red dashed line) and EDst variation (green solid line), (c) two pair stations method, using the pair of DAV and MND for the daily range (grey solid line) and EUEL (red dashed line).

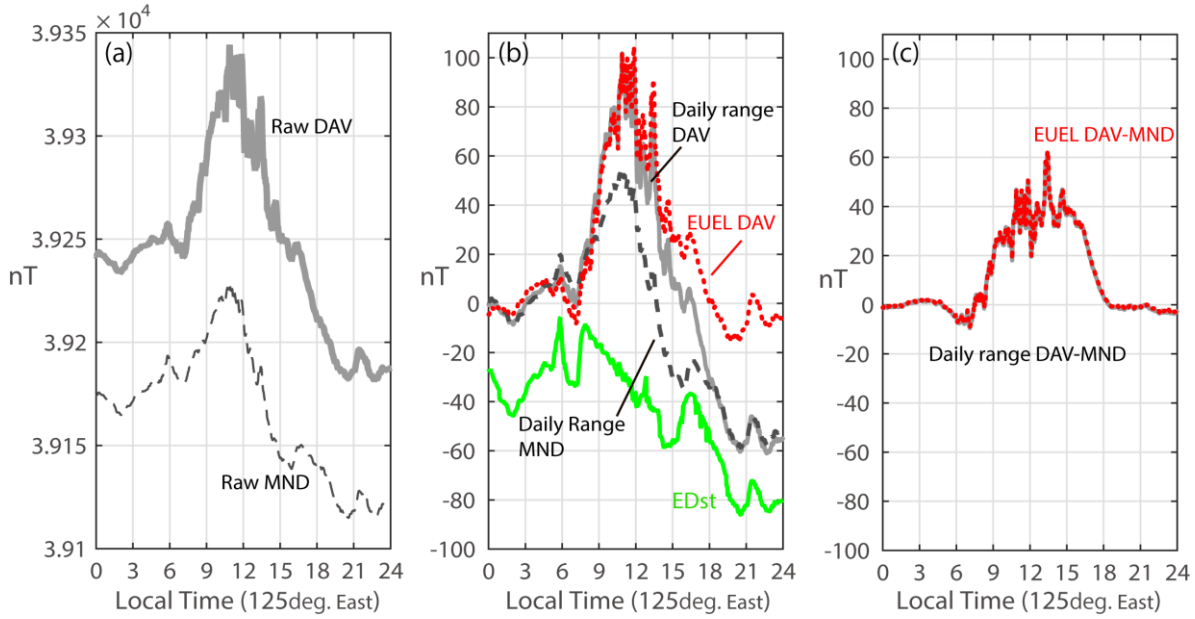

Figure 4: Schematic illustration of the daily range method, EE-index and two pair stations method during the geomagnetic disturbance time as the same manner of Figure 2, on 15th February 2012 in the local time (125 degrees east longitude), from February 14 (1540 UT) to 15 (1539 UT), 2012.

In contrast, for the magnetic disturbance time (Figure 4 (b)), there is noticeable difference between the daily range method and EUEL of EE-index. EUEL removes successfully the magnetic effect of magnetospheric current, as EDst, from the original observational magnetic field data. Therefore, the nighttime EUEL variation roughly exists around zero. Two midnights level neighboring the day considered are widely different, since the magnetic variation of the daily range remains the magnetic effect of the magnetospheric currents. The results suggest that EE-index is the useful indicator during the magnetic disturbance time.

Fortunately, the pair of stations is available for isolating EEJ effect from the Sq variation. The behavior of two pair method is also presented for the example of the isolation of EEJ variation from Sq variation in Figure 3 (c) and 4 (c). The grey line is calculated by using DAV and MND of the daily range. The red dashed line is obtained by subtracting $EUEL_{MND}$ from $EUEL_{DAV}$. There is no outstanding difference between two methods. Note that the appropriate station pair may not always exist for applying to two stations pair method.

Using the improved EE-index, the time series analysis (the line chart and the spectral analysis) are executed for EUEL at ANC and the solar activity from September 18, 1998 to March 31, 2015 in this paper, in order to reveal influences of the solar activity on the EEJ intensity throughout one solar cycle. The solar radio emission at 10.7 cm (F10.7) is used in our analysis as the indicator of solar activity. F10.7 data are obtained from the GSFC/SPDF OMNIWeb interface at http://omniweb.gsfc.nasa.gov (King and Papitashvili, 2005). We used Dst value (provided by WDC of Kyoto University) as EDst from 1998 to 2004, because there are few stations for determining EDst during these periods. As evaluated by Uozumi et al. (2008), this substitution is reasonable for the long-term analysis. In this paper, the term "daily EEJ peak" is used to refer to the maximum of the dayside EUEL intensity. Note that we analyze not EEJ variations but the total equatorial magnetic field on the magnetic equator. The EEJ intensity is typically maximum around 1100 LT during the low sunspot year and around 1200 LT during the high sunspot year (Rastogi and Iyer, 1976). Hence the daily EEJ peak is selected between 1000 and 1400 LT for the individual day. The parameters used in the spectral analysis for daily EEJ peak (1-day sampling rate) are as follows: 2-year FFT window with the humming window and sliding 30 days along the time series.

Results

Figure 5 (a) and (b) show the hourly averaged EUEL intensity in color coding for UT hour (vertical axis) and day (horizontal axis, tick labels are given by year) and F10.7 for day (horizontal axis, the same manner of EUEL tick labels). Comparing Figure 5 (a) and 5 (b), it is obvious that the long-term trend of EUEL intensity corresponds to F10.7. The variability in F10.7 shows two peaks of the solar activity during the analyzed interval. One is around 2002 in solar cycle 23 (1996 - 2008), the other is around 2014 in solar cycle 24 (2009 -). The peak of F10.7 in solar cycle 23 is larger than the peak in solar cycle 24. The similar peaks and the long-term trend are found in the EUEL intensity around the local noon (1500 -1800 UT), which are denoted with warm color (Figure 5 (a)).

In order to see the relationship between F10.7 and the intensity of the daily EEJ peak during local noon, we demonstrated the time series plot (line chart) of both F10.7 and the daily EEJ peak in Figure 5 (c). The temporal day-to-day F10.7 variations are different from

the daily EEJ peak. The fluctuation in the long-term of F10.7 has a tendency to increase with increase of the value of F10.7, whereas the daily EEJ peak consists of the long-term trend and the irregular fluctuation.

The results of the spectral analysis are shown in Figure 6. The power spectrum of the daily EEJ peak has clearly two dominant peaks throughout the analysis interval in the left panel: 14.5 days and 180 days (semi-annual), which correspond to lunar tides (Gasperini and Forbes, 2014) and the Russell-McPherron Effect (Russell and McPherron, 1973), respectively. In contrast, F10.7 power spectrum shows no continuous peaks through solar cycles (the right panel in Figure 6).

The daily EEJ peak power spectrum is stronger around the solar maximum years than the solar minimum years. In other words, there is a lack of spectrum power between 2007 and 2009 except for the frequency of the lunar tides and semi-annual variations. A similar tendency appears in F10.7 power spectrum for all of frequencies.

We extended the analysis for the solar cycle dependence in both F10.7 and the daily EEJ peak. Figure 7 (a) shows the 540 days running averaged daily EEJ peak and F10.7, in order to remove lower period variations (for example day-to-day, solar rotation, annual and semi-annual variations) from the daily EEJ peak and F10.7. The grey line in Figure 7 (a) shows the intensity 1.4 times the smoothed daily EEJ peak values shifted downward by 80. The solar cycle variations of amplified daily EEJ peak (the grey line) have a good correlation with that of F10.7, with the correlation coefficient 0.99.

The subtraction of long-period trends from the daily EEJ peak and F10.7 variations is shown in the bottom panel of Figure 7 (b). The differences of F10.7 significantly depend on the solar cycle: F10.7 differential values increase during the solar maximum years and decrease during the lower solar activity. The daily EEJ peak differential variations (the black line) show the dominant semi-annual variations (the yellow line results from calculating the 81 days running average in order to removing the lower period variations than semi-annual period). There are solar cycle modulations of semi-annual daily EEJ peak variations. The semi-annual variability slightly depends on the solar activity.

Discussion

The results of our analysis are as follows:

1. The long-term variation of daily EEJ peak intensity has a trend similar to that of F10.7 (the solar activity).
2. The dominant spectrum powers of daily EEJ peak occur at 14.5 days and 180 days throughout two solar cycles. In contrast, F10.7 has no dominant spectrum peaks throughout the analyzed interval.
3. The solar cycle variation of daily EEJ peak correlates well with that of F10.7 (the correlation coefficient 0.99).

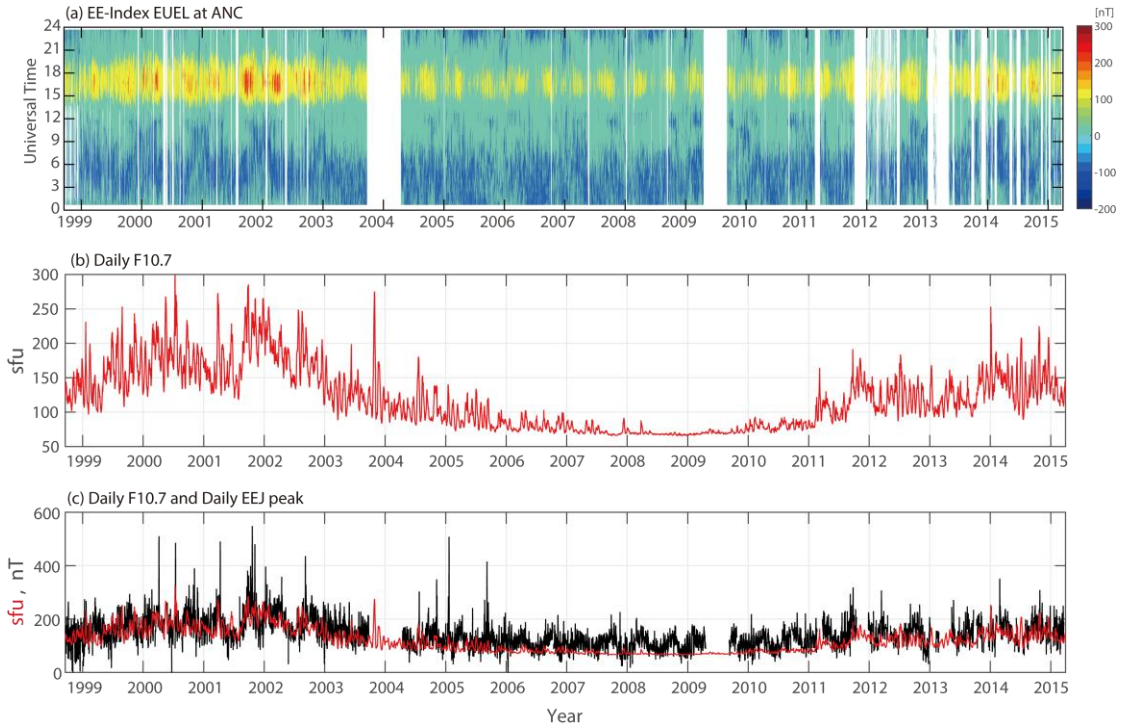

Figure 5 : The long-term variations of EUEL/daily EEJ peak and F10.7. (a) the hourly averaged EUEL intensity in color coding for UT hour (vertical axis) and year (horizontal axis), (b) F10.7 for year (horizontal axis) and (c) the time series plot (line chart) of both daily F10.7 and the daily EEJ peak. In (a), the lack of data is denoted with white color. 1 sfu = 10^{-22}Wm^{-2}Hz^{-1}.

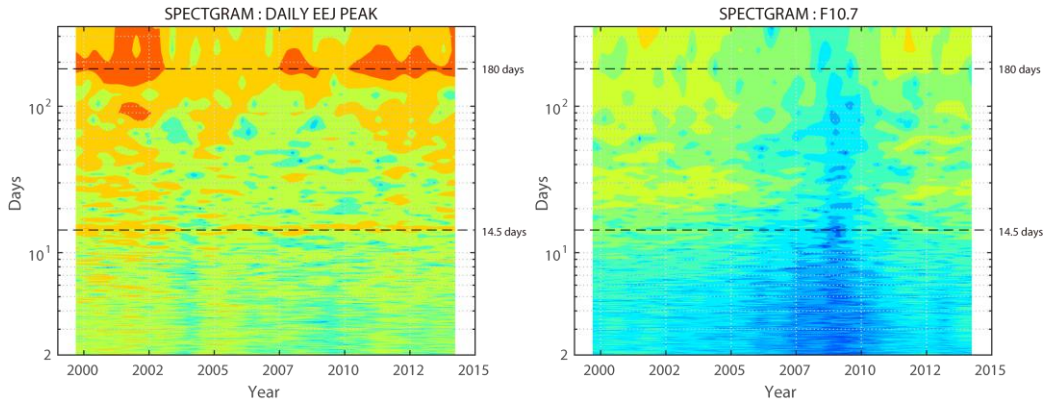

Figure 6: A dynamic spectrum from 1999 to 2014. The left panel shows the power spectrum of daily EEJ peak. The right panel is F10.7. The horizontal dash lines denote the 14.5 days and 180 days.

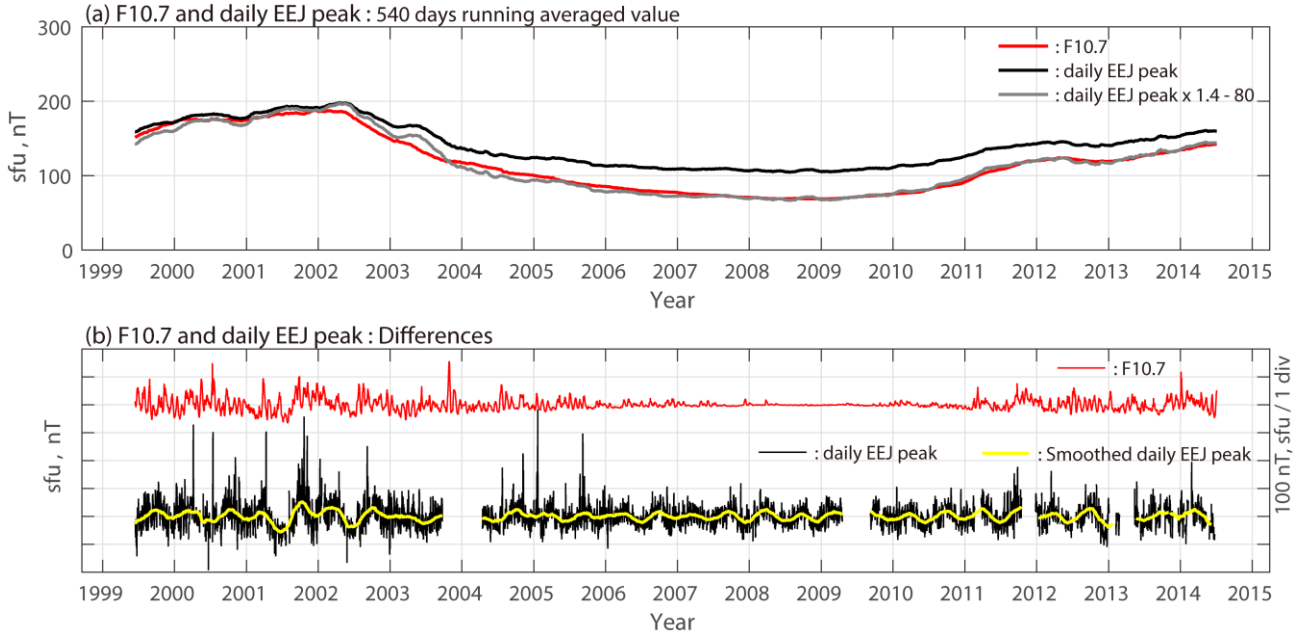

Figure 7: Long-period variations of daily EEJ peak and F10.7. (a) is the 540-days running averaged values and (b) shows the differences of them from the daily value. In both panels, the red and black line indicates daily F10.7 and the daily EEJ peak, respectively. In the panel (a), the grey line represents the daily EEJ peak intensity 1.4 times the smoothed daily value shifted downward by 80. In the panel (b), the yellow line indicates the smoothed daily EEJ peak value by calculating the 81 days running average.
1 sfu = 10^{-22}Wm^{-2}Hz^{-1}.

Hamid et al. (2013) showed that the EEJ intensity represented by the difference of EUEL between dip-equator and off-dip stations had a similar long-period trend of the solar F10.7 flux through one year during 2011. The long-term trend variations of EEJ, which is similar to the solar cycle variation of F10.7, are found by using the successive time series data in the present paper. In contrast, the day-to-day variation of daily EEJ peak correlates poorly with daily F10.7. These results suggest that the long-period solar activity mainly controls the trend of long-term variation in the intensity of daily EEJ peak. It is well known that the solar activity has an 11-year cycle and the effect of the solar cycle appears into the quantities representing the solar activity such as the solar radiation (Hathaway, 2010, for a review).

The 14.5-day and semi-annual variations has strong power spectrum throughout solar cycles, whereas these F10.7 variations has no signal in Figure (6). This suggests that two variations of EEJ relate poorly to the solar radiation and other sources control these EEJ variations. The predominant sources are the lunar tides (Gasperini and Forbes, 2014) and the Russell-McPherron Effect (Russell and McPherron, 1973) for 14.5-day and semi-annual variations, respectively. Lunar tide variations contribute to the ionospheric electric field changes.

The day-to-day EEJ variations seem to be controlled by other parameters related to the atmosphere rather than F10.7 (solar radiation). Yamazaki et al. (2014) found that the day-to-day EEJ variations during magnetic quiet periods are mainly controlled by the response of the zonal polarization electric field to variable zonal winds. Recently many possible explanations are proposed for the long-period trend and the day-to-day variations of EEJ in terms of

atmospheric dynamics. The EEJ current is described by the Cowling conductivity (Hirono, 1950a, 1950b) and the eastward current along the dip-equator caused by the tidal winds. The tidal winds and temperature variations are well known to be attributed with the solar activity (Forbes, 1978). Additionally the thermospheric density and ionospheric electron density decrease with decreasing the solar EUV irradiance (Liu et al., 2006; Solomon et al., 2010). Because both decreasing density leads to lower Cowling conductivity, the EEJ intensity decreases. We need to further analyze the contribution of the atmospheric dynamics to EEJ in future work.

The daily EEJ peak often has a large amplitude (> 400 nT) as shown Figure 5 (c). We found that these amplified EEJ peaks correspond to magnetic storms. Because the main topic of our analysis is the long-period EEJ variations, we does not give detailed discussions for such transient disturbances .There are uncertainties of the EE-index during the main phase of magnetic storms. The EE-index will be needed to improve this matter.

We conclude that the daily EEJ peak intensity is roughly determined as the summation of the long-period trend of the solar activity resulting from the solar cycle and day-to-day variations caused by various sources such as lunar tides, geometric effects, magnetospheric phenomena and atmospheric phenomena. Many past studies demonstrate the similarity between EEJ and F10.7, although that are provided from the monthly averaged values calculated by using solar quiet days (Rastogi and Iyer, 1976; Rastogi, Alex, and Patil, 1994). The EE-index allows us to study the EEJ variations in terms of the time series analysis with high time resolution, regardless of the geomagnetic environment (magnetic quiet/disturbance). This work presents the primary evidence for solar cycle variations of EEJ by using the long-term study of the EE-index. The real-time EE-index is published on the web of ICSWSE for the purpose of monitoring the equatorial magnetic variation involving EEJ.

Acknowledgments

We wish to acknowledge that this paper was originally presented at "2015 UN/Japan Workshop on Space Weather". This event was supported in part by JSPS Core-to-Core Program (B. Asia-Africa Science Platforms), Formation of Preliminary Center for Capacity Building for Space Weather Research. We thank World Data Center (WDC) for Geomagnetism Kyoto University for providing geomagnetic indices Dst. We thank Goddard Space Flight Center/Space Physics Data Facility (GSFC/SPDF) OMNIWeb at http://omniweb.gsfc.nasa.gov for providing F10.7 solar radiation data. Special thanks are due to the Ocean Hemisphere network Project (OHP), University of Tokyo for providing with the CXI magnetometer data. The PI of MAGDAS/CPMN project, A. Yoshikawa, ICSWSE, Kyushu Univ. very much appreciates 32 organizations and Co-investigators around the world for their ceaseless cooperation and contribution to the MAGDAS/CPMN project. The MAGDAS observation is financially supported by Japan Society for the Promotion of Science (JSPS) as Grant-in-Aid for Overseas Scientific Survey (15253005, 18253005). The MAGDAS/CPMN database is also supported by JSPS for Publication of Scientific Research Results (128068, 138059, 148071, 158068, 168066, 188068, 198055, 208043), and National Institute of Information and Communications Technology (NiCT) as funded research. This work was supported by JSPS KAKENHI Grant Number 15H05815.

References

Chapman, S. and Raja Rao, K.S.: 1965, J. Atmos. Terr. Phys., 27, 559, doi:10.1016/0021-9169(65)90020-6.

Doumouya, V., Cohen, Y., Arora, B.R. and Yumoto, K.: 2003, J. Atmos. Solar-Terrestrial Phys., 65, 1265, doi:10.1016/j.jastp.2003.08.014.

Doumouya, V., Vassal, J., Cohen, Y., Fambitakoye, O. and Menvielle, M.: 1998, Ann. Geophys., 16, 658, doi:10.1007/s005850050637.

Fambitakoye, O. and Mayaud, P.N.: 1976a, J. Atmos. Terr. Phys., 38, 1, doi:10.1016/0021-9169(76)90188-4.

Fambitakoye, O. and Mayaud, P.N.: 1976b, J. Atmos. Terr. Phys., 38, 19, doi:10.1016/0021-9169(76)90189-6.

Fambitakoye, O., Mayaud, P.N. and Richmond, A.D.: 1976, J. Atmos. Terr. Phys., 38, 113, doi:10.1016/0021-9169(76)90118-5.

Forbes, J.M.: 1978, J. Geophys. Res., 83, 3691, doi:10.1029/JA083iA08p03691.

Forbes, J.M.: 1981, Rev. Geophys., 19, 469, doi:10.1029/RG019i003p00469.

Gasperini, F. and Forbes, J.M.: 2014, Geophys. Res. Lett., 41, 3026, doi:10.1002/2014GL059294.

Hamid, N., Liu, H., Uozumi, T., Yumoto, K., Veenadhari, B., Yoshikawa, A. and Sanchez, J.: 2014, Earth, Planets Sp., 66, 146, doi:10.1186/s40623-014-0146-2.

Hamid, N.S.A., Liu, H., Uozumi, T. and Yumoto, K.: 2013, Antarct. Rec., 57, 329.

Hathaway, D.H.: 2010, Living Rev. Sol. Phys., 7, doi:10.12942/lrsp-2010-1.

Hirono, M.: 1950a, J. Geomagn. Geoelectr., 2, 1, doi:10.5636/jgg.2.113.

Hirono, M.: 1950b, J. Geomagn. Geoelectr., 2, 113, doi:10.5636/jgg.2.113.

Kane, R.P. and Trivedi, N.B.: 1980, J. Atmos. Terr. Phys., 42, 303, doi:10.1016/0021-9169(80)90038-0.

King, J.H. and Papitashvili, N.E.: 2005, J. Geophys. Res. Sp. Phys., 110, 1, doi:10.1029/2004JA010649.

Liu, L., Wan, W., Ning, B., Pirog, O.M. and Kurkin, V.I.: 2006, J. Geophys. Res., 111, A08304, doi:10.1029/2006JA011598.

Onwumechili, A.: 1967, Physics of Geomagnetic Phenomena, Academic Press, New York, p. 425-507.

Rastogi, R.G., Alex, S. and Patil, A.: 1994, J. Geomagn. Geoelectr., 46, 115, doi:10.5636/jgg.46.115.

Rastogi, R.G., Chandra, H. and Yumoto, K.: 2013, Earth, Planets Sp., 65, 1027, doi:10.5047/eps.2013.04.004.

Rastogi, R.G. and Iyer, K.N.: 1976, J. Geomagn. Geoelectr., 28, 461, doi:10.5636/jgg.28.461.

Rigoti, A., Chamalaun, F.H., Trivedi, N.B. and Padilha, A.L.: 1999, Earth, Planets Sp., 51, 115.

Russell, C.T. and McPherron, R.L.: 1973, J. Geophys. Res., 78, 92, doi:10.1029/JA078i001p00092.

Sabaka, J.T., Olsen, N. and Purucker, M.E.: 2004, Geophys. J. Int., 159, 521, doi:10.1111/j.1365-246X.2004.02421.x.

Solomon, S.C., Woods, T.N., Didkovsky, L. V., Emmert, J.T. and Qian, L.: 2010, Geophys. Res. Lett., 37, 1, doi:10.1029/2010GL044468.

Uozumi, T., Yumoto, K., Kitamura, K., Abe, S., Kakinami, Y., Shinohara, M., Yoshikawa, A., Kawano, H., Tamiki, U., Terumasa, T., McNamara, D., Ishituka, J.K., Dutra, S.L.G., Damtie, B., Doumbia, V., Obrou, O., Rabiu, A.B., Adimula, I.A., Othman, M., Fairos, M., Otadoy, R.E.S. and the MAGDAS group: 2008, Earth, Planets Sp., 60, 785, doi:10.1186/BF03352828.

Yamazaki, Y., Richmond, A.D., Maute, A., Liu, H.-L., Pedatella, N. and Sassi, F.: 2014, J. Geophys. Res. Sp. Phys., 119, 6966, doi:10.1002/2014JA020243.

Yumoto, K. and the CPMN group: 2001, Earth, Planets Sp., 53, 981.

Yumoto, K. and the MAGDAS group: 2006, , in N. Gopalswamy, A. Bhattacharyya (eds.), Proceedings of the ILWS Workshop, Quest Publications for ILWS and Indian Institute of Geomagnetism, Goa, India, p.399.

Yumoto, K. and the MAGDAS group: 2007, Bull. Astron. Soc. India, 35, 511.